Removal of naproxen and diclofenac using an aquaporin hollow fiber forward osmosis module

Irena Petrinic[a,*], Hermina Bukšek[a], Ildikó Galambos[b], Renáta Gerencsér-Berta[b], Marshall S. Sheldon[c], Claus Helix-Nielsen[a,d]

[a]*University of Maribor, Faculty of Chemistry and Chemical Engineering, Smetanova ulica 17, 2000 Maribor, Slovenia,
emails: irena.petrinic@um.si (I. Petrinic), hermina.buksek@um.si (H. Bukšek)*
[b]*University of Pannonia, Soós Ernő Water Technology and Research Center, H-8800 Nagykanizsa, Zrínyi M. Str. 18, Hungary,
emails: galambos.ildiko@sooswrc.hu (I. Galambos), berta.renata@sooswrc.hu (R. Gerencsér-Berta)*
[c]*Cape Peninsula University of Technology, Department of Chemical Engineering, P.O. Box: 1906, Bellville 7535, South Africa,
email: SheldonM@cput.ac.za (M.S. Sheldon)*
[d]*Technical University of Denmark, Department of Environmental Engineering, Bygningstorvet, Building 115, 2800 Kgs. Lyngby,
Denmark, email: clhe@env.dtu.dk (C. Helix-Nielsen)*

ABSTRACT

The rejection of trace organic contaminants, contained in model solutions, was investigated using an osmotically driven membrane filtration process. Two compounds naproxen (NAP) (0.1–0.88 mg/L), and diclofenac sodium (DIC-Na) (0.39–1.55 mg/L) and a mixture (where concentrations for NAP were 0.57–0.81 mg/L and for DIC-Na 0.39–0.46 mg/L) were selected for this study as the feed solutions (FS). The draw solutions (DS) were 1 and 2 M NaCl, respectively. Forward osmosis filtrations were carried out using an aquaporin inside membrane hollow fiber forward osmosis lab-module. The average water flux was 12 and 24 LMH while an average reverse salt flux was 2 and 6 GMH for 1 and 2 M NaCl DS and deionized water as FS, respectively. When filtrating NAP, DIC-Na, and the mixture, the highest flux was achieved with the DIC-Na followed by NAP and the mixture and were more pronounced using 2 M NaCl solution as a DS. From the rejection results, it can be concluded that DIC was completely rejected both in its solution and in the mixtures, while NAP rejection varied from 98.4% and 98.8% for 1 and 2 M NaCl and 98.8% in the mixture when 2 M NaCl was used as a DS.

Keywords: Forward osmosis; AIM™ hollow fibre lab-module; Naproxen and diclofenac sodium rejection

1. Introduction

Trace organics contaminants (TrOCs) constitute a group of synthetic compounds that have been detected recently in trace amounts in surface waters [1]. Naidu et al. [2] reported that the main source of drugs in the environment (surface water) is human and animal excreta products of medical treatment. These compounds are subjected to a process of metabolic degradation in the human and animal organism. However, significant fractions of the original substances are expelled in the form of active metabolites or non-metabolized forms in the urine and feces [3]. The therapeutic group of nonsteroidal anti-inflammatory drugs is the most abundant, with naproxen (NAP) and diclofenac (DIC) as the molecules most frequently found and detected in the highest environmental concentrations [4].

These compounds are not easily degradable by conventional biological treatment processes [5], which is usually

* Corresponding author.

the fundamental principle of conventional wastewater treatment plants [6]. However, it was reported that conventional activated sludge, as common biological wastewater treatment, could effectively remove biodegradable TrOCs like ibuprofen and bisphenol A [7]. Advanced oxidation processes (AOPs), such as Fenton, photo-Fenton, Fenton-like, and electrochemical oxidation processes are also considered as effective methods in the degradation of different TrOCs. These methods, being non-selective, have high removal efficiency, and can completely remove most of the pollutants depending on the conditions and contact time. However, high energy and chemical requirements are major economic limitations for these AOPs as well as incomplete degradation of TrOCs can lead to the production of some intermediate substances during the reaction, which may potentially be more toxic than the initial compounds [8].

As an emerging membrane technology, forward osmosis (FO) can supply high-quality water by utilizing a natural osmotic pressure gradient to extract water from a feed solution (FS) into a draw solution (DS), and can offer unique merits such as reduced pressure operation, low fouling propensity, excellent solute rejection, and relatively low energy consumption if proper regeneration/separation of the DS is achieved but reversely diffuses the draw solutes towards the FSs [9]. Since the composition of the DS can be tailored depending on the application, FO may have advantages when compared to energy-intense pressure-driven filtration processes, such as reverse osmosis (RO) [10]. The effect of the DS and membrane material on FO membrane rejection of TrOCs has been evaluated and a high reverse salt flux (RSF) of used DS (0.07–0.1 M NaCl) hindered the adsorption and diffusion of the TrOCs in the membrane material [11] resulting in a higher TrOCs rejection efficiency compared to RO [12]. Numerous studies focusing on the rejection of TrOCs by FO membranes have all indicated high levels of rejection both in bench and pilot-scale [13–16]. Overall, the rejection mechanisms are similar to that for NF/RO membranes and governed mostly by size exclusion (steric interactions) and electrostatic interactions. The affinity of specific organics molecules towards the FO membrane, for example, through hydrophobic interactions, may also influence the rejection, particularly when the solute is comparable or smaller than the effective pore size of the FO membrane [17].

Jin et al. [18] investigated the rejection of TrOCs by two different types of FO membranes, cellulose triacetate (CTA) and thin-film composite (TFC) membranes. The transport of TrOCs through the benchmark CTA membranes was found to be mainly governed by steric interactions, with hydrophobic and electrostatic interactions playing minor roles. For example, charged TrOCs with a large hydrated radius have consistently shown lower permeability in CTA membranes than neutral TrOCs [19]. On the other hand, TFC membranes have shown better overall rejections due to improved membrane physicochemical properties such as greater negative surface charge, more hydrophobic character, and smaller hydrated pore sizes [20].

For applications that require space-saving and lightweight design (portable FO systems) as well as large volume separations, the compact (high packing density) hollow fiber (HF) membrane configuration may, therefore, be advantageous [21]. A recent FO membrane, commercially available in an HF configuration, is the aquaporin inside membrane (AIM™). These membranes are based on the use of aquaporins which are naturally occurring protein water channels in proteins where the proteins are an integral part of the membrane structure [22,23]. High rejection rates for small size trace organics were reported using small scale flat sheet AIM™ FO coupons [10], as well as larger-scale HF AIM™ modules [24]. Madsen et al. [10] compared the pesticide removal performances of commercial Hydration Technology Innovations LLC (HTI) membrane and flat sheet AIM™ membrane. The AIM™ membrane was capable of rejecting atrazine, 2,6-dichlorobenzamide and desethyl-desisopropyl atrazine (DEIA) up to 97%, outperforming the HTI FO membrane especially in rejecting small neutral compounds like DEIA. The rejection by the HTI membrane was controlled by steric hindrance while the rejection by the AIM™ membrane was controlled by diffusion of the trace organics through the membrane. As expected, the AIM™ membrane exhibited a significantly higher flux than the HTI membrane. Similarly, Engelhardt et al. [24] investigated the rejection of 2,4-dichlorophenoxyacetic acid (2,4-D), bisphenol A (BPA) and methylparaben using AIM™ hollow fiber forward osmosis (HFFO) (0.6 m²) module where the AIM™ membrane rejected over 95% of methylparaben and over 99% for 2,4-D and BPA.

However, to our knowledge, no study exists that investigates the FO membrane rejection characteristics of TrOCs mixtures. Here we investigated the performance of an AIM™ HFFO lab module (active area 180 cm²) for concentrating NAP, diclofenac sodium (DIC-Na) solutions, and a mixture (NAP/DIC-Na) with 1 and 2 M NaCl as DS. The rejection efficiency, water flux as well as RSF were evaluated at an average pH of 5. This work not only opens a new insight into FO membrane rejection of isolated TrOCs but also provides information about the competitive permeation effects of TrOC mixtures.

2. Materials and methods

2.1. Materials

Napmel 500 mg (used for NAP solution) tablets were purchased from PannonPharma (Hungary) and Diclofenac-Ratiopharm 50 mg tablets (used for DIC-Na solution) from Teva Pharmaceutical Industries, Hungary. The chemical structures and physicochemical properties of NAP and DIC-Na are presented in Table 1 [25–27].

2.2. Sample preparation

Synthetic NAP solutions were prepared from 500 mg Napmel tablets which were pulverized and diluted in methanol/deionized (DI) water = 50/50 ratio, while the DIC-Na solution was prepared from 50 mg Diclofenac-Ratiopharm tablets pulverized and diluted in 45/55 acetonitrile/DI water solution.

Stock solutions for NAP (1 g/L): two tablets containing 1000 mg of NAP, were ground. 100 mg of grained tablets were dissolved in 100 mL of solvent (methanol/DI water = 50/50 ratio). Stock solutions for DIC-Na (1 g/L): two tablets contained 100 mg of DIC-Na, were ground and dissolved in 100 mL of solvent (acetonitrile/DI water = 45/55).

With further appropriate dilution, 1 mg/L of NAP and DIC-Na were used for filtrations.

Measured values for used FS and DS in this study are presented in Table 2.

2.3. Analyses

A Zetasizer Nano-S (Malvern Instruments, Malvern, UK) was used to obtain the zeta potential of the particles [28] by application of the Henry equation as well as the hydrodynamic diameter and size distribution. The osmolality of the solutions was determined via freezing-point depression (Gonotec, cryoscopic osmometer – OSMOMAT 030, Germany) and the osmotic pressure, π was determined [29].

2.4. Membrane used

The specification of the AIM™ HFFO lab-module used in the study is given in Table 3.

The zeta potential (ζ) of the membrane surface was determined by streaming potential measurements with an electrolyte solution of 1.0 mM KCl using an electrokinetic analyzer (SurPASS, Anton Paar GmbH, Austria) at various pH values (Fig. 1). Despite the complex geometry of the HFFO membrane bundles in the lab-scale module, a good reproducibility was observed for the inner membrane surface.

2.5. Experimental set-up of FO filtrations

The experimental set-up is composed of a peristaltic pump (Longer Pump® BT 100–1, flow rates from 0.002 to 175 mL/min, China) a weighing scale (OHAUS Scout-pro 4000 g, USA), a stirrer, two different solutions (FS and DS), the HF membranes integrated with the membrane module, and a conductivity meter (SD 320 Con, Lovibond, Germany). The weighing scale and conductivity meter were connected to a laptop to enable automatic recording of the FS weight and conductivity. The schematic of the FO process is shown in Fig. 2a and the AIM™ HFFO lab-module used in Fig. 2b.

The cross-flow velocity used for experiments was 120 ml/min. The volumes used were 0.5 L for FS and 0.25 L for DS. During the filtration, the samples of both the FS and DS were taken at 0, 30, and 60 min for high-performance liquid chromatography (HPLC) analyses.

Water flux, J_w (LMH) across the membrane were calculated using Eq. (1) [31]:

$$J_w = \frac{\Delta V}{A\,\Delta t} \tag{1}$$

where ΔV is the total volume change of permeate water (L), A is the effective membrane area (m²) and Δt is the time (h).

The RSF, J_s (GMH) was determined using Eq. (2) [31]:

$$J_s = \frac{\gamma_t V_t - \gamma_0 V_0}{A\,\Delta t} \tag{2}$$

where γ_0 is the initial concentration of the FS (g/L), V_0 is the initial volume of the FS (L), γ_t is the solute concentration (g/L), V_t is the volume of the FS measured at the time (L), Δt is the time (h) and A is the effective membrane area (m²).

Total dissolved solids (g/L) of the FS, which serve as mass concentration γ_t and γ_0 in Eq. (2), were determined using Eq. (3) [32]:
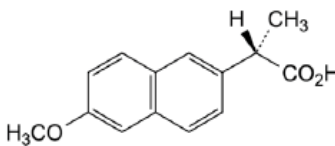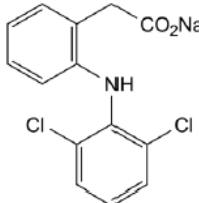
$$TDS = k \times \kappa \tag{3}$$

where k is the correlation factor (0.4804 for NaCl) and κ is the conductivity of the FS (μS/cm).

The rejection rates of the TrOCs (NAP, DIC-Na) were calculated by using the initial FS parameters and final DS parameters using Eq. (4) [33]:

$$R(\%) = \left(1 - \frac{\gamma_{fd} \times V_{fd}}{\gamma_{id} \times V_{id}}\right) \times 100 \tag{4}$$

where γ_{fd} is the mass concentration in the final DS (g/L); V_{fd} is the volume of the final DS (L); γ_{if} is the mass

Table 1
Structure of NAP and DIC-Na and their physicochemical properties

	NAP	DIC-Na
IUPAC name	(2S)-2-(6-methoxynaphthalen-2-yl) propanoic acid	sodium 2-{2-[(2,6-dichlorophenyl)amino]phenyl} acetate
M_W (Da)	230.26	318.13
$\log K_{ow}$	3.18	4.51
pKa	4.15	4.15
$\log D$ pH = 7	2.88	4.55

concentration in the initial FS (g/L) and V_{if} is the volume of the initial FS (L).

In this experiment, the final volume of the DS instead of permeate volume was used to calculate the concentration of DS as permeated water was mixed with the initial DS in the process.

2.6. Liquid chromatography

HPLC measurements were performed on an XBridge C18 column 3.5 μm, 4.6 mm × 50 mm, produced by waters (Milford, USA). The column and sample temperature was 20°C precision of ±1°C. Eluents used were acetonitrile (ACN) (VWR, USA) and 0.1% formic acid (VWR, USA) with a gradient grade elution of 1 mL/min. The timesheet was 0 min 40% ACN, 10 min 60% ACN, and 12 min 40% ACN. 10 μL of the FS samples were injected and 100 μL for the DS with a delay of 2 min between each injection. The detector is a diode array used at two wavelengths: 230 nm for NAP and 277 nm for DIC-Na. The software used to process all the data was to Empower 2 software. The detection limit was 0.01 mg/L.

3. Results and discussion

3.1. Baseline measurements

During 1 h of operation with DI water as an FS, water flux and RSF were measured for 1 and 2 M NaCl solutions as a DS.

Table 2
Characteristics of used FS and DS solutions

	Solutions used	pH	π (bar)	d (nm)	ZP (mV)
FS	NAP	4.9	0.198	529.3	−21.6
	DIC-Na	5.1	0.297	1,541.5	−16.05
	NAP/DIC-Na	5.0	0.495	591.3	−28.1
DS	1 M NaCl	5.76	44.3	–	–
	2 M NaCl	5.63	88.0	–	–

Table 3
Specification of the AIM™ HFFO lab-module [30]

| Membrane lab-module	AIM™ HFFO
Manufacturer	Aquaporin A/S (Kongens Lyngby, Denmark)
Module dimensions	130 mm in length, 17 mm in diameter
Active area (lumen side/shell side)	0.018 m²
Number of fibers	300
Fiber length	110 mm
Inner diameter of fibers	195 μm
Wall thickness	35 μm
Fibre material	Polysulfone/polyvinylpyrrolidone (PS/PVP)
Active layer	Thin-film composite (TFC) with embedded aquaporin proteins
Water flux (DI water vs. 1 M NaCl)	>12 L/m²h (LMH)
Reverse salt flux (DI water vs. 1 M NaCl)	<2 g/m²h (GMH)
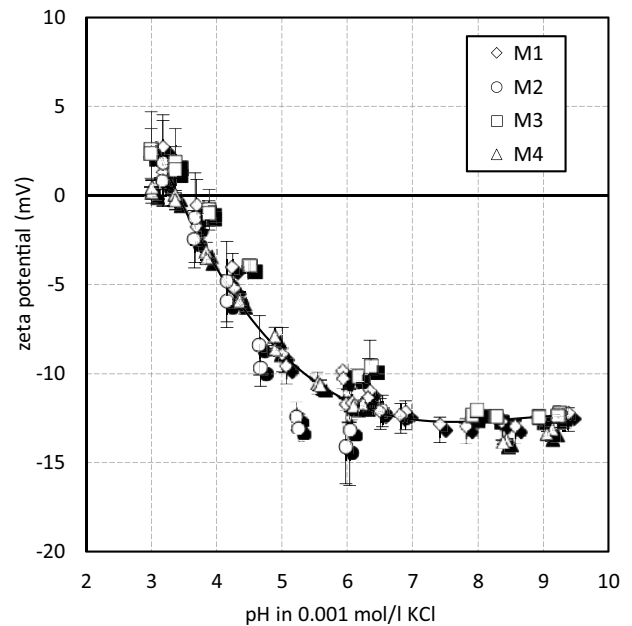
Fig. 1. Zeta potential of a pristine AIM™ HFFO membrane vs. pH.

Fig. 3 shows curves that illustrate the average values of the six individual measurements.

From these six individual experiments, two refer to pre and post-filtration of NAP, DIC-Na, and NAP/DIC-Na, respectively. All sets of experiments were performed using one AIM™ HFFO lab-module that was cleaned after each cycle of the experiment. For cleaning, the FS and DS solutions were DI water for 15 min, after which both FS and DS compartments were filled with 1L of DI water and the recirculation of both solutions was performed and left to run for another 15 min.

During FO operation, a decrease in water flux is normally observed with time. The occurrence of concentration polarization and dilution of DS by permeation water concertedly contributed to the decrease in osmotic pressure difference.
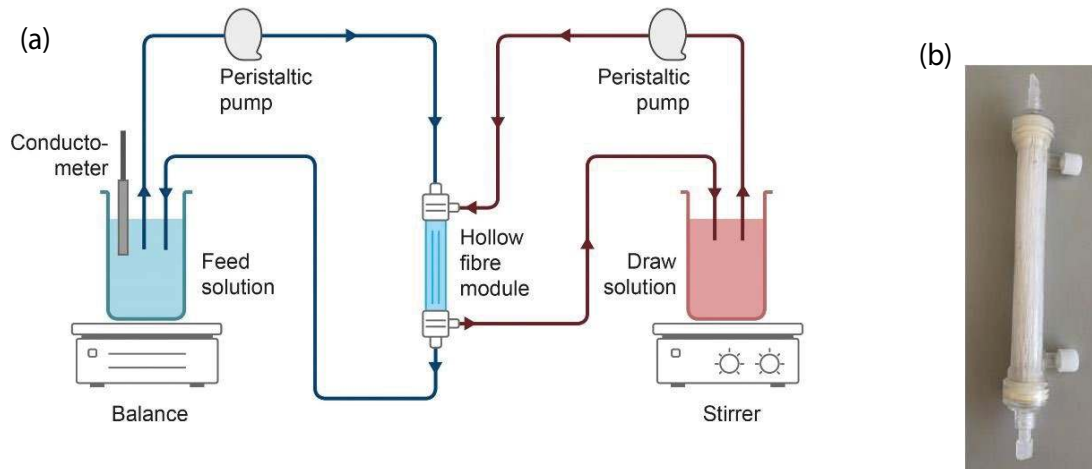
Fig. 2. (a) Schematic illustration of the FO setup and (b) photo of the used AIM™ HFFO lab-module.
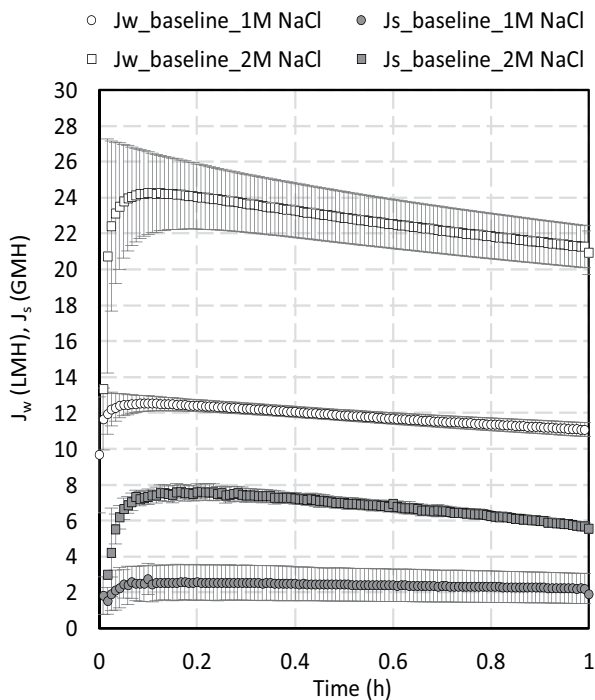

Fig. 3. Baseline performance for AIM™ HFFO lab-module: FS (DI water); DS (1 and 2 mol/L NaCl, respectively). The measurement is based on the average values of six measurements with standard deviation.

From Fig. 3, it can be seen that the highest J_w value was 12.54 ± 0.44 LMH at the beginning of filtration and dropped to 11.08 ± 0.39 LMH after 1 h of filtration when 1 M NaCl was used as DS. Similar data for an average FO water flux of approximately 13.2 LMH for 1 M NaCl DS and DI feed water for AIM™ HFFO was reported by Ren and McCutcheon [34].

Generally, a larger throughput is preferred as it improves the efficiency of the filtration. The increment in water flux was achieved by using a more concentrated DS. As can be observed, when using 2 M NaCl as a DS, a higher concentration gradient as the driving force was achieved which not only generates a high water flux but also diffuses more DS into the FS. In the case of 2 M NaCl, the flux was 24.26 ± 2.22 LMH at the beginning of filtration and dropped to 20.93 ± 1.21 LMH at the end of 1 h filtration. Following J_s value was 2.75 ± 0.87 GMH at the beginning of filtration, followed by 1.91 ± 0.88 GMH at the end of 1 h filtration for 1 M NaCl whiles for 2 M NaCl, J_s is 7.63 ± 0.41 GMH at the start of filtration reaching 5.56 ± 0.08 GMH at the end of 1 h filtration. The specific RSF (J_s/J_w) is a quantitative indicator for bi-directional diffusion in the FO process. Higher specific RSF reflects a decrease in the selectivity of the membrane and a lower process efficiency [35]. For the 1 M NaCl DS solution it was 0.22 g/L and for 2 M NaCl 0.3 g/L, respectively.

3.2. Effect of NAP, DIC-Na and its mixture solutions on filtration

Each experiment using NAP, DIC-Na, and NAP/DIC-Na consisted of five sequential steps: baseline (Fig. 3), cleaning, filtration, cleaning, and final (second) baseline.

Table 4
The concentration of NAP alone in FS and DS and rejection for 1 and 2 M NaCl, respectively

	FS = NAP, DS = 1 M NaCl			FS = NAP, DS = 2 M NaCl		
t (min)	γ in FS (mg/L)	γ in DS (mg/L)	Rejection (%)	γ in FS (mg/L)	γ in DS (mg/L)	Rejection (%)
0	0.88	/	/	0.9	/	/
30	0.97	0.02	98.6	1.1	0	100
60	1.10	0.02	98.4	1.41	0.01	98.8

Three FS consisting of either NAP, DIC-Na, or the NAP/DIC-Na mixture at an initial concentration given in Tables 4–7 were operated with 1 M NaCl and 2 M NaCl as a DS, respectively (Figs. 4a–f)).

Figs. 4a and b present J_w and J_s and conductivity increase (κ) with time for NAP solution and baseline before and after the filtration during 1 h with 1 and 2 M NaCl as a DS, respectively. J_w for filtration and baseline is almost the same which indicates that no fouling occurred. However, there is a difference in conductivity of FSs for baselines before and after the NAP filtration, which is not seen in J_s values as well as for the conductivity increase during the NAP filtration. This might be due to solutes trapped inside the membrane or adsorbed at the membrane surface. If the cleaning is not done completely, the trapped or adsorbed FS or DS solutes slowly and gradually diffuse out and contribute to the increasing J_s values. When using 2 M NaCl as DS; a higher concentration gradient generates higher J_w, J_s, and conductivity values compared to 1 M NaCl as DS (Fig. 4). However, here the conductivity increases for Baseline 1 and 2 are similar. The same set of results, for DIC-Na and NAP/DIC-Na solutions, are presented in Figs. 4c and d and Figs. 4e and f, respectively.

Filtrations for NAP, DIC-Na alone in solution, and NAP/DIC-Na mixture are collected together and presented in Figs. 5a and b with J_w and κ as well as average baselines presented with J_w, J_s and κ (as shown in Fig. 3) for 1 and 2 M NaCl as DS, respectively.

Fouling is more pronounced when having 2 M NaCl as DS since there is a higher drop in J_w and a higher difference in J_w among each FS used. The highest flux was achieved with the DIC-Na follow by NAP solutions and NAP/DIC-Na mixture and more pronounced using 2 M NaCl solution as a DS (Fig. 5b). A previous study evaluated the performance of a polyamide-imide HF membrane [36] that demonstrated high water permeability and salt rejection. The charges in the densely active membrane surface were found to impose a repulsive force on salt penetration through the membrane. The same effect was observed when filtrating the DIC-Na solution, where a higher flux was observed when using both 1 and 2 M NaCl, as a DS. The pKa value of DIC-Na is 4.15 (same as NAP), however, DIC-Na is negatively charged at pH > 4.2. The rejection can be explained by repulsion of the negatively charged DIC-Na and the negative charge membrane surface of the AIM™ HFFO lab-module.

Table 5
The concentration of DIC-Na alone in FS and DS and rejection for 1 and 2 M NaCl, respectively

	FS = DIC-Na, DS = 1 M NaCl			FS = DIC-Na, DS = 2 M NaCl		
t (min)	γ in FS (mg/L)	γ in DS (mg/L)	Rejection (%)	γ in FS (mg/L)	γ in DS (mg/L)	Rejection (%)
0	0.52	/	/	0.55	/	/
30	1.52	0	100	1.65	0	100
60	2.18	0	100	2.20	0	100

Table 6
The concentration of NAP and DIC-Na (in FS and DS) and rejection in the NAP/DIC-Na mixture for 1 M NaCl

	FS = Mixture NAP/DIC-Na, DS = 1 M NaCl					
	NAP			DIC-Na		
t (min)	γ in FS (mg/L)	γ in DS (mg/L)	Rejection (%)	γ in FS (mg/L)	γ in DS (mg/L)	Rejection (%)
0	0.57	/	/	0.39	/	/
30	1.30	0	100	0.85	0	100
60	1.59	0	100	1.62	0	100

Table 7
The concentration of NAP and DIC-Na (in FS and DS) and rejection in the NAP/DIC-Na mixture for 2 M NaCl

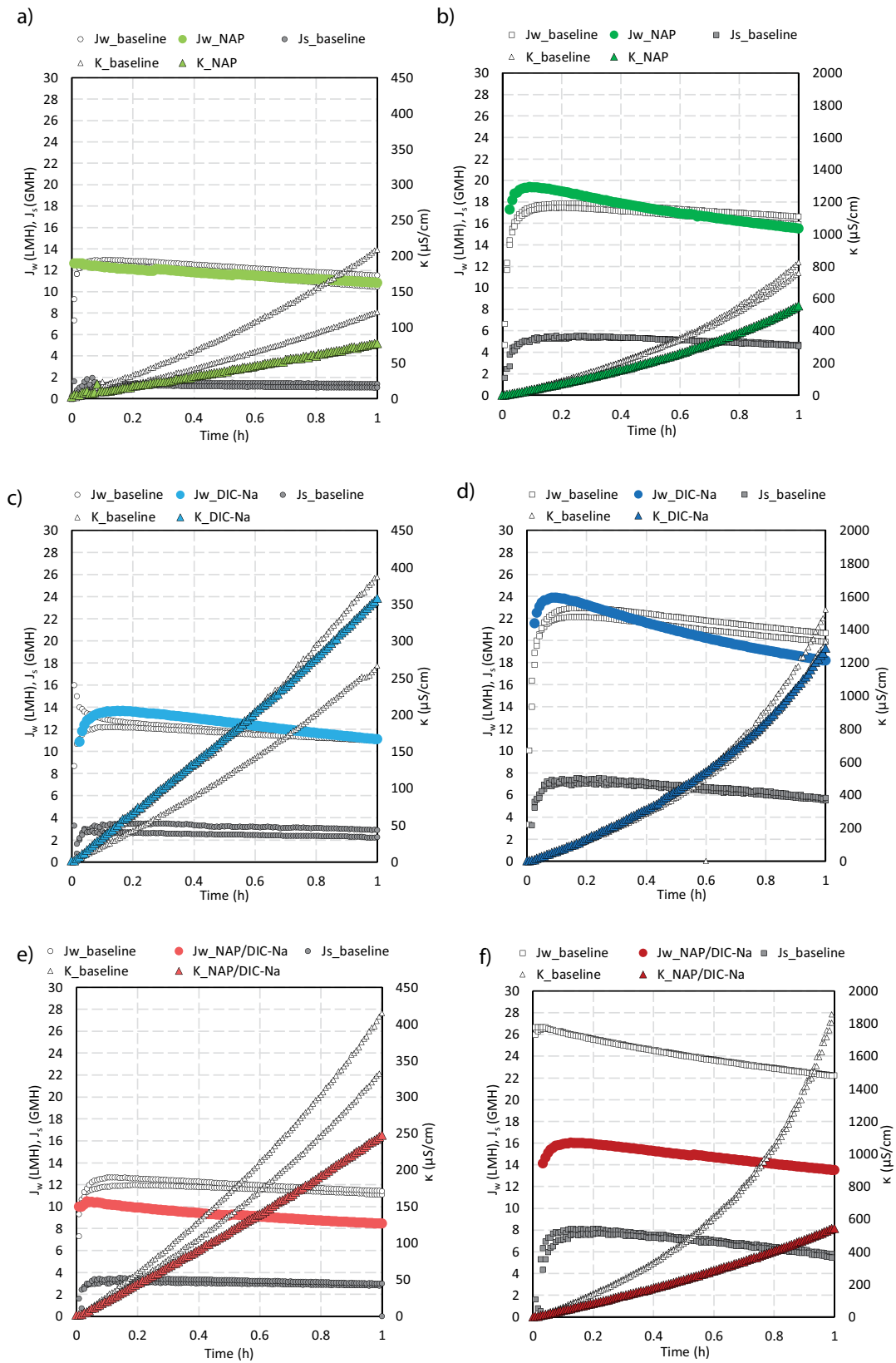|	FS = Mixture NAP/DIC-Na, DS = 2 M NaCl					
	NAP			DIC-Na		
t (min)	γ in FS (mg/L)	γ in DS (mg/L)	Rejection (%)	γ in FS (mg/L)	γ in DS (mg/L)	Rejection (%)
0	0.81	/	/	0.46	/	/
30	1.67	0	100	1.56	0	100
60	2.16	0.01	98.8	1.89	0	100

Fig. 4. Filtration performance (J_w, J_s and κ (conductivity increase)) of the AIM™ HFFO lab-module for (a) FS: NAP, DS: 1 mol/L NaCl; (b) FS: NAP, DS: 2 mol/L NaCl; (c) FS: DIC-Na, DS: 1 mol/L NaCl; (d) FS: DIC-Na, DS: 2 mol/L NaCl; (e) FS: NAP/DIC-Na, DS: 1 mol/L NaCl; (f) FS: NAP/DIC-Na, DS: 2 mol/L NaCl. Colored curves (empty symbols) are presented for κ: (a) and (b) for NAP in green, (c) and (d) for DIC-Na in blue and (e) and (f) NAP/DIC-Na in red for 1 and 2 M NaCl, as DS respectively.
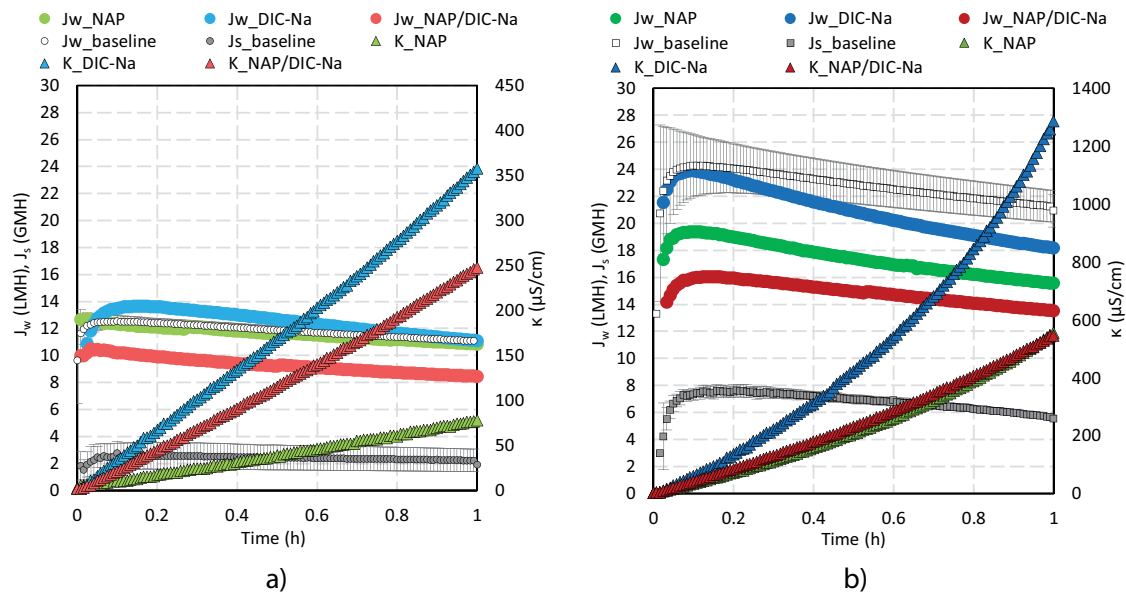
Fig. 5. Filtration performance of AIM™ HFFO lab-module: (a) FS: NAP, DIC-Na or NAP/DIC-Na and DS: 1 mol/L NaCl and (b) FS: NAP, DIC-Na or NAP/DIC-Na and DS: 2 mol/L NaCl.

3.3. Effect of TrOCs transport behavior on rejection

The effects on the rejection of NAP and DIC-Na alone and the mixture of NAP/DIC-Na using 1 and 2 M NaCl were studied. The concentration and rejection data for NAP, DIC-Na alone for 1 and 2 M NaCl DS are given in Tables 4 and 5, respectively.

From the rejection results, it is evident that NAP permeates through the AIM™ HFFO lab-module whilst DIC-Na is completely rejected. NAP (pKa 4.15) molecules at pH 4.0 and 5.0 were mainly in the non-dissociated form [37] whilst DIC-Na is negatively charged at pH > 4.2. Thus rejection can be explained by repulsion of the negatively charged DIC-Na and the negative charge membrane surface of the AIM™ HFFO lab-module. With the increase of pH, the zeta-potential is decreased (Fig. 1).

Concentrations of NAP and DIC-Na (in FS and DS) in the mixture of NAP/DIC-Na are given in Table 6 and Table 7 for 1 and 2 M NaCl, respectively.

Experiments were conducted to investigate whether there is a competitive permeation effect of NAP and DIC-Na at given initial concentrations (Tables 4 and 5). When using 1 M NaCl as DS NAP was completely rejected. With 2 M NaCl as DS, NAP was completely rejected initially, however, permeation was seen after 1 h of filtration. This could be due to a higher initial concentration of NAP as well as in higher water flux (Fig. 5b). A similar rejection result is observed for NAP at a given initial concentration of 0.9 mg/L when 2 M NaCl is used as DS (Table 4). DIC-Na at given initial concentrations of 0.39 and 0.46 mg/L in the mixture was 100% rejected when 1 and 2 M NaCl DS were used as an FS.

4. Conclusions

The study of FO filtration of NAP and DIC-Na and the mixture at different initial concentrations of FS showed that the highest flux was achieved with the DIC-Na follow by NAP solutions and NAP/DIC-Na mixture and were more pronounced using 2 M NaCl solution as a DS. From the rejection results, it can be concluded that DIC-Na is completely rejected both in its solution and in the mixtures, while NAP rejection varied from 98.4% and 98.8% for 1 and 2 M NaCl and 98.8% in the mixture when 2 M NaCl was used as a DS.

Acknowledgment

References

[1] J. Zhang, B. Sun, X.M. Xiong, N.Y. Gao, W.H. Song, E.D. Du, X.H. Guan, G.M. Zhou, Removal of emerging pollutants by Ru/TiO₂-catalyzed permanganate oxidation, Water Res., 63 (2014) 262–270.
[2] R. Naidu, A.V. Arias Espana, Y.J. Liu, J. Jit, Emerging contaminants in the environment: risk-based analysis for better management, Chemosphere, 154 (2016) 350–357.
[3] B. Tiwari, B. Sellamuthu, Y. Ouarda, P. Drogui, R.D. Tyagi, G. Buelna, Review on fate and mechanism of removal of pharmaceutical pollutants from wastewater using biological approach, Bioresour. Technol., 224 (2017) 1–12.
[4] N.H. Tran, M. Reinhard, K. Yew-Hoong Gin, Occurrence and fate of emerging contaminants in municipal wastewater treatment plants from different geographical regions-a review, Water Res., 133 (2018) 182–207.
[5] S. Tewari, R. Jindal, Y.L. Kho, S. Eo, K. Choi, Major pharmaceutical residues in wastewater treatment plants and receiving waters in Bangkok, Thailand, and associated ecological risks, Chemosphere, 91 (2013) 697–704.
[6] C. Grandclément, I. Seyssiecq, A. Piram, P. Wong-Wah-Chung, G. Vanot, N. Tiliacos, N. Roche, P. Doumenq, From the conventional biological wastewater treatment to hybrid

processes, the evaluation of organic micropollutant removal: a review, Water Res., 111 (2017) 297–317.

[7] S. Suárez, M. Carballa, F. Omil, J.M. Lema, How are pharmaceutical and personal care products (PPCPs) removed from urban wastewaters?, Rev. Environ. Sci. Bio/Technol., 7 (2008) 125–138.

[8] M. Malhotra, S. Suresh, A. Garg, Tea waste derived activated carbon for the adsorption of sodium diclofenac from wastewater: adsorbent characteristics, adsorption isotherms, kinetics, and thermodynamics, Environ. Sci. Pollut. Res., 25 (2018) 32210–32220.

[9] S.Q. Zou, Z. He, Enhancing wastewater reuse by forward osmosis with self-diluted commercial fertilizers as draw solutes, Water Res., 99 (2016) 235–243.

[10] H.T. Madsen, N. Bajraktari, C. Hélix-Nielsen, B. Van der Bruggen, E.G. Søgaard, Use of biomimetic forward osmosis membrane for trace organics removal, J. Membr. Sci., 476 (2015) 469–474.

[11] M. Sauchelli, G. Pellegrino, A. D'Haese, I. Rodríguez-Roda, W. Gernjak, Transport of trace organic compounds through novel forward osmosis membranes: role of membrane properties and the draw solution, Water Res., 141 (2018) 65–73.

[12] S.W. Kim, K.H. Chu, Y.A.J. Al-Hamadani, C.M. Park, M. Jang, D.-H. Kim, M. Yu, J. Heo, Y.M. Yoon, Removal of contaminants of emerging concern by membranes in water and wastewater: a review, Chem. Eng. J., 335 (2018) 896–914.

[13] B.D. Coday, B.G.M. Yaffe, P. Xu, T.Y. Cath, Rejection of trace organic compounds by forward osmosis membranes: a literature review, Environ. Sci. Technol., 48 (2014) 3612–3624.

[14] A.A. Alturki, J.A. McDonald, S.J. Khan, W.E. Price, L.D. Nghiem, M. Elimelech, Removal of trace organic contaminants by the forward osmosis process, Sep. Purif. Technol., 103 (2013) 258–266.

[15] M. Xie, L.D. Nghiem, W.E. Price, M. Elimelech, Comparison of the removal of hydrophobic trace organic contaminants by forward osmosis and reverse osmosis, Water Res., 46 (2012) 2683–2692.

[16] N.T. Hancock, P. Xu, D.M. Heil, C. Bellona, T.Y. Cath, Comprehensive bench- and pilot-scale investigation of trace organic compounds rejection by forward osmosis, Environ. Sci. Technol., 45 (2011) 8483–8490.

[17] L.D. Nghiem, T. Fujioka, Removal of Emerging Contaminants for Water Reuse by Membrane Technology, N.P. Hankins, R. Singh, Eds., Emerging Membrane Technology for Sustainable Water Treatment, Elsevier Science, Amsterdam, Netherlands, 2016, pp 217–247.

[18] X. Jin, J. Shan, C. Wang, J. Wei, C.Y. Tang, Rejection of pharmaceuticals by forward osmosis membranes, J. Hazard Mater., 227–228 (2012) 55–61.

[19] A. D'Haese, Dissertation, Mechanistic Modeling of Mass Transport Phenomena in Forward Osmosis, Ghent University, Belgium, 2017.

[20] M. Xie, L.D. Nghiem, W.E. Price, M. Elimelech, Relating rejection of trace organic contaminants to membrane properties in forward osmosis: measurements, modelling and implications, Water Res., 49 (2014) 265–274.

[21] P.S. Goh, A.F. Ismail, B.C. Ng, M.S. Abdullah, Recent progresses of forward osmosis membranes formulation and design for wastewater treatment, Water, 11 (2019) 2043.

[22] J.Y.M. Tang, S. McCarty, E. Glenn, P.A. Neale, M.S.J. Warne, B.I. Escher, Mixture effects of organic micropollutants present in water: towards the development of effect-based water quality trigger values for baseline toxicity, Water Res., 47 (2013) 3300–3314.

[23] Y. Zhao, C. Qiu, X. Li, A. Vararattanavech, W. Shen, J. Torres, C. Helix-Nielsen, R. Wang, X. Hu, A.G. Fane, C.Y. Tang, Synthesis of robust and high-performance aquaporin-based biomimetic membranes by interfacial polymerization-membrane preparation and RO performance characterization, J. Membr. Sci., 423–424 (2012) 422–428.

[24] S. Engelhardt, A. Sadek, S. Duirk, Rejection of trace organic water contaminants by an aquaporin-based biomimetic hollow fiber membrane, Sep. Purif. Technol., 197 (2018) 170–177.

[25] F.X. Kong, H.W. Yang, Y.G. Wu, X.M. Wang, Y.F. Xie, Rejection of pharmaceuticals during forward osmosis and prediction by using the solution–diffusion model, J. Membr. Sci., 476 (2015) 410–420.

[26] N. Lindqvist, T. Tuhkanen, L. Kronberg, Occurrence of acidic pharmaceuticals in raw and treated sewages and in receiving waters, Water Res., 39 (2005) 2219–2228.

[27] L. Estelle, R. Ayman, J.Å. Jönsson, Sludge removal of nonsteroidal anti-inflammatory drugs during wastewater treatment studied by hollow fiber liquid phasemicro extraction, J. Environ. Prot., 4 (2013) 946–955.

[28] M. Kaszuba, J. Corbett, F.M. Watson, A. Jones, High-concentration zeta potential measurements using light-scattering techniques, Philos. Trans. R. Soc. London, Ser. A, 368 (2010) 4439–4451.

[29] I. Ban, S. Markus, S. Gyergyek, M. Drofenik, J. Korenak, C. Helix-Nielsen, I. Petrinic, Synthesis of poly-sodium-acrylate (PSA)-coated magnetic nanoparticles for use in forward osmosis draw solutions, Nanomaterials, 9 (2019) 1238.

[30] S. Engelhardt, J. Vogel, S.E. Duirk, F.B. Moore, H.A. Barton, Urea and ammonium rejection by an aquaporin-based hollow fiber membrane, J. Water Process Eng., 32 (2019) 100903.

[31] S.H. Oh, S.J. Im, S. Jeong, A. Jang, Nanoparticle charge affects water and reverse salt fluxes in forward osmosis process, Desalination, 438 (2018) 10–18.

[32] F. Rusydi, Correlation between conductivity and total dissolved solid in various type of water: a review, IOP Conf. Ser.: Earth Environ. Sci., 118 (2018) 012019.

[33] H. Lee, S.-J. Im, J. Hyoung Park, A. Jang, Removal and transport behavior of trace organic compounds and degradation byproducts in forward osmosis process: effects of operation conditions and membrane properties, Chem. Eng. J., 375 (2019) 122030.

[34] J. Ren, J.R. McCutcheon, A new commercial biomimetic hollow fiber membrane for forward osmosis, Desalination, 442 (2018) 44–50.

[35] N. Hancock, T.Y. Cath, Solute coupled diffusion in osmotically driven membrane processes, Environ. Sci. Technol., 43 (2009) 6769–6775.

[36] S.A. Yousefi, M.S. Nasser, I.A. Hussein, S. Judd, Influence of polyelectrolyte architecture on the electrokinetics and dewaterability of industrial membrane bioreactor activated sludge, J. Environ. Manage., 233 (2019) 410–416.

[37] G. Li, R. Deng, G. Peng, C. Yang, Q. He, Y. Lu, H. Shi, Magnetic solid-phase extraction for the analysis of bisphenol A, naproxen and triclosan in wastewater samples, Water Sci. Technol., 77 (2018) 2220–2227.